JOURNAL OF Materials CHEMISTRY

Preparation of whisker penetrated ceramics by internal precipitation of hollandite within a tielite matrix

Sandro Kohn[a] and Martin Jansen*[a,b]†

[a] *Institut für Anorganische Chemie, Gerhard-Domagk-Str. 1, 53121 Bonn, Germany*
[b] *Max-Planck-Institut für Festkörperforschung, Heistenbergstr. 1, 70569 Stuttgart, Germany*

Composite ceramics consisting of tielite (Al_2TiO_5) as the prevailing phase and potassium hollandite ($K_2Al_2Ti_6O_{16}$) have been prepared by internal precipitation from amorphous solids having the appropriate compositions. The formation of the two crystalline phases from a starting material made *via* a sol–gel process, through reaction sintering, or through a glass ceramic process has been studied by X-ray diffraction, ^{27}Al MAS NMR spectroscopy, DTA–TG and SEM–EDX. It has been shown that the hollandite phase crystallises as whiskers within the tielite matrix. The approach reported presents an alternative route for the production of whisker reinforced materials.

Introduction

Ceramic materials have many desirable properties. However, their brittleness is a severe drawback that has not been met satisfactorily, so far. There have been various attempts to minimise the consequences of this drawback. One well known strategy is to reinforce the ceramic material by adding whiskers as toughening agents. Whiskers are needle-shaped single crystals with nearly theoretical strength due to their perfect geometry.[1] The reinforcement by the whiskers is usually traced back to their ability to span a developing crack and to absorb fracture energy. Commonly such a composite is synthesised by producing whiskers and powders of the matrix materials separately, then mixing them and applying conventional powder processing to this mixture. Alumina reinforced by silicon carbide whiskers[2] and silicon nitride reinforced by silicon carbide whiskers[3] are well known examples for this approach. The synthesis and the characterisation of silicon carbide whiskers are described in ref. 4.

In this study we intended to extend the concept of internal whisker precipitation[5] as a route to reinforced ceramics. The basic idea of the approach presented is to create the matrix as well as the whisker phase simultaneously by an annealing process. In this way, the expensive synthesis of sometimes carcinogenic whiskers is circumvented, and the internal crystal growth is expected to lead to a microstructure with flaws smaller in size and fewer in number.

In principle the concept of internal whisker precipitation can be realised *via* three different routes; (1) a sol–gel process and subsequent annealing, (2) reaction sintering and (3) a glass ceramic process.

During sol–gel and glass ceramic processes a glassy-amorphous solid is synthesised in a first step by hydrolysis of suitable precursors or by melting and quenching appropriate compositions of the starting materials. While annealing the glassy samples in a second step, both matrix and whisker phases crystallise. Using the process of reaction sintering crystalline powder mixtures react directly in the solid state without producing a non-crystalline intermediate.

To verify the approach of internal phase precipitation we selected tielite Al_2TiO_5 as a matrix material. Tielite is the only known ternary phase in the quasi-binary system Al_2O_3–TiO_2.[6] Aluminium titanate is of considerable interest for technical applications because of its excellent thermal shock resistance. However, tielite ceramics do not have wide technical importance as yet due to their insufficient mechanical stability. This low mechanical strength of tielite is caused by the different coefficients of thermal expansion in the different crystallographic directions ($a=-2.9\times10^{-6}$ K^{-1}, $b=11\times10^{-6}$ K^{-1}, $c=18\times10^{-6}$ K^{-1})[7] leading to microcracking after sintering.[8,9] An additional problem is the eutectic decomposition into corundum and rutile in the temperature range from 800–1300 °C.[10,11] In order to tackle this drawback numerous authors[12,13] have discussed and tried to chemically stabilise aluminium titanate by introducing other metal oxides (SiO_2, MgO, *etc.*). In a more recent patent application[14] reinforcement of tielite by SiC whiskers applying the usual powder processing has been reported.

A tendency for needle-shaped crystal growth is an essential requirement for the internal precipitation of a whisker phase. As a rule, this is the case if one lattice constant is much smaller than the other two. From this point of view hollandites seem to be promising candidates because of their small c/a ratio in the tetragonal crystal system. Hollandites[15,16] form a large family of structures with the general composition $[A_x][B_yC_{8-y}]O_{16}$. The A cations residing in channels of the $[B_yC_{8-y}]O_{16}$ framework are comparatively big and can be mono- (K, Na, Ag, Rb, Tl) or divalent (Sr, Ba, Pb). The smaller [B, C] cations constituting the octahedral framework can be di-, tri-, tetra- or pentavalent (Mg, Cu, Zn, Co, Ni, Al, Ga, Fe, In, Cr, Si, Ge, Ti, Mn, Sn, Sb). We have selected the potassium hollandite $K_2Al_2Ti_6O_{16}$[17–19] as a potentially whisker forming phase. By this choice the number of components of the final system is kept low.

Suitable compositions of the desired composites include any ratio of Al_2TiO_5 to $K_2Al_2Ti_6O_{16}$. In the concentration triangle

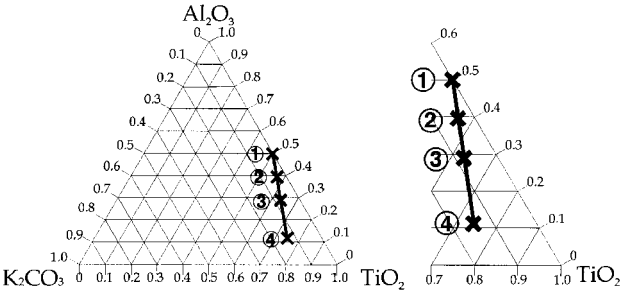

Fig. 1 Concentration triangle of the system K_2CO_3–Al_2O_3–TiO_2; enlarged part showing the quasi-binary section from tielite Al_2TiO_5 to potassium hollandite $K_2Al_2Ti_6O_{16}$. The marked positions 1, 2, 3 and 4 represent the ratios 1:0, 10:1, 3:1 and 0:1, respectively.

†E-mail: m_jansen@snchemie2.chemie.uni-bonn.de

(Fig. 1) all these compositions are realised along the line fixed by the two boundary compositions Al_2TiO_5 and $K_2Al_2Ti_6O_{16}$. This section of compositions is of particular interest, as all compositions aside from this line would lead to ceramics containing additional phases which are assumed to have unfavourable effects on the properties of the ceramic.

In a first step the conditions of formation and the crystallisation behaviour of the pure phases aluminium titanate and potassium hollandite were examined. From the composite ceramics those with a tielite (T):potassium hollandite (H) ratio of 3:1 to 10:1, in integral steps, were studied in detail.

Experimental section

Sample characterisation

All samples were characterised at different stages of processing by X-ray powder diffraction, ^{27}Al MAS NMR spectroscopy, DTA–TG and SEM–EDX analysis.

X-Ray powder diffraction patterns were recorded on a diffractometer (STADI P, Stoe & Cie, Darmstadt) using a position sensitive detector ($6° \leqslant 2\theta \leqslant 80°$; 0.1° steps; Cu-K$\alpha_1$). Reference powder X-ray diffraction data were obtained from the JCPDS database (version 1.20, September 1996).

^{27}Al MAS NMR spectroscopy was performed on a Unity 400 spectrometer (Varian, Darmstadt) using a 9.4 Tesla superconducting magnet; 1 μs pulse lengths and 1 s delay times were applied to collect single pulse spectra at spinning frequencies of 10 kHz.

DTA–TG analyses were carried out on a DTA apparatus (STA 429, Netzsch, Darmstadt) in a highly purified argon atmosphere with a heating rate of 5 °C min^{-1} using corundum crucibles (particle size of the samples 5–500 nm).

SEM was performed on a microscope (DSM 940, Zeiss, Oberkochen) operated at 25 kV accelerating potential. The microscope was equipped with an energy dispersive X-ray analysis system (EDAX PV 9800, Röntgenanalytik, Taunusstein). Selected bulk samples were polished with silicon carbide abrasive paper and with 6 and 1 μm diamond pastes. All samples were gold-coated in order to avoid charging.

Sample preparation and processing

Sol–gel process. Hydrolysis of well homogenised solutions of appropriate metal alkoxides is a suitable way to produce amorphous sol–gel powders. For the system K–Al–Ti–O metal isopropylates are particularly advantageous, because aluminium isopropylate and titanium isopropylate are commercially available and potassium isopropylate is easily accessible by reacting potassium with isopropanol. Stoichiometric amounts of the starting alkoxides as solutions in isopropanol $\{c[Al(OPr^i)_3] = 0.15\ mol\ l^{-1};\ c[Ti(OPr^i)_4] = 1\ mol\ l^{-1};\ c(KOPr^i) = 1.19\ mol\ l^{-1}\}$ were refluxed for 2 h under highly purified argon and subsequently hydrolysed by exposing the solution to air overnight. The products consisted of finely divided, colourless and amorphous powders. After preheating the gels at 500 °C for 48 h powder pellets of the samples were annealed according to the temperature programs as given in Table 1.

The last column in Table 1 specifies the process identified by X-ray diffraction. Crystallisation from an amorphous state (C) is discerned from the formation (F) of a phase as a result of a solid state reaction of crystalline phases. After crystallisation and formation, respectively, crystal growth (CG) is achieved by heating at elevated temperatures.

Reaction sintering. The starting mixtures were prepared by ball milling (isopropanol dispersion, 15 min) of corundum, rutile and potassium carbonate in the respective compositions. The batches were heated for 24 h at 150 °C. Residues of isopropanol were removed by vacuum drying overnight. Powder pellets of these starting mixtures were sintered according to the temperature programs given in Table 2.

Glass ceramic process. The powder mixtures of starting materials (for their pre-treatment see preceding paragraph, Table 2) were melted in an induction furnace, applying an average heating rate of 10 °C min^{-1}, under a slight flow of highly purified argon (flow rate = 0.5 l min^{-1}) at temperatures of 1650–1900 °C. The experimental set-up consisted of a boron nitride crucible, closed by a lid, which was placed inside a cylindrical graphite susceptor. This system was protected against the atmosphere by placing it inside a water cooled reaction tube of quartz glass. The temperature was measured pyrometrically at the surface of the graphite susceptor. The samples were quenched by switching off the furnace and pouring liquid nitrogen into the reaction quartz tube. The average cooling rate was about 70 °C s^{-1}.

Results and Discussion

Sol–gel process

DTA–TG, X-ray diffraction. In order to determine the crystallisation temperatures the gels were analysed by DTA–TG and X-ray diffraction; this procedure is described for sample 4. Fig. 2 shows the DTA–TG plot of the sol–gel powder 4. For all samples a weight loss of 25–30% was detected, depending on the degree of predrying. The first endothermic peak at about 124 °C is due to the removal of associated water. The following broad exothermic peak is attributed to the decomposition of organic residues. This process is finished at about 450 °C. XRD analysis shows the material to be amorphous up

Table 1 Compositions studied, by the sol–gel route, batches of 15 g; temperature programs used for annealing the sol–gel samples, heating rates: 200 °C h^{-1}

batch	T:H	mol% Al_2O_3	mol% TiO_2	mol% K_2CO_3 (K_2O)	T/°C	holding time/h	process (products identified)
1	1:0	50.0	50.0	—	800	12	C (K, R)
					1200	24	CG (K, R)
					1400	48	F (T)
2	10:1	39.3	57.1	3.6	800	12	C (H, A, R)
					900	12	C (K)
					1200	24	CG (K, R)
					1400	48	F (T)
3	3:1	28.6	64.3	7.1	800	12	C (H, A, R)
					900	12	C (K)
					1200	24	CG (K, R)
					1400	48	F (T)
4	0:1	12.5	75.0	12.5	700	12	C (H)
					1200	24	CG (H)

T = tielite; H = potassium hollandite; K = corundum; A = anatase; R = rutile. C = crystallisation; F = formation; CG = crystal growth.

Table 2 Starting mixtures as studied by reaction sintering, batches of 15 g; processing of the batches obtained *via* reaction sintering, heating rates: 200 °C h^{-1}

batch	T:H	mol% Al_2O_3	mol% TiO_2	mol% K_2CO_3	T/°C	holding time/h	process (products identified)
1	1:0	50.0	50.0	—	1400	48	F (T)+CG (T)
2	10:1	39.3	57.1	3.6	1100	12	F (H)
					1200	24	CG (H)
					1480	48	F (T)+CG (T)
3	3:1	28.6	64.3	7.1	1100	12	F (H)
					1200	24	CG (H)
					1480	48	F (T)+CG (T)
4	0:1	12.5	75.0	12.5	1100	12	F (H)
					1200	48	CG (H)

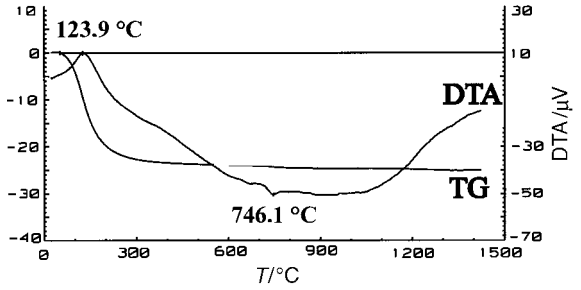

Fig. 2 DTA–TG plot of sol–gel powder 4; the effects at 123.9 and 746.1 °C are attributed to the removal of associated water and to the crystallisation of potassium hollandite

to 700 °C (Fig. 3), thus proving that the sample remains amorphous after the removal of the associated water and the organics. The following exothermic peak at 746 °C corresponds to the crystallisation of potassium hollandite as recorded independently by X-ray diffraction. Table 3 summarises the crystallisation temperatures as detected by DTA analysis and X-ray diffraction.

During the crystallisation processes potassium hollandite and tielite behave quite differently. While potassium hollandite crystallises directly from the amorphous matrix, tielite is formed in a two-step process. Rutile and corundum are formed first and then react in a solid state reaction yielding aluminium titanate (Table 3). In the presence of potassium a partial crystallisation of anatase precedes the formation of rutile, and the reaction of corundum with rutile forming tielite starts at a higher (by 100 °C) temperature (Table 3). During subsequent annealing of the powder pellets (see Experimental section, Table 1) this elevated reaction temperature was considered.

^{27}Al MAS NMR spectroscopy. Fig. 4 shows ^{27}Al MAS NMR spectra representative of the sol–gel powder 3 before and after preheating at 500 °C for 24 h. The signal width in each spectrum proves the samples to be amorphous in agreement with the results of X-ray diffraction and DTA–TG. Both samples show the presence of fourfold, fivefold and sixfold coordinated aluminium (Al^{IV}: $+50 \leqslant \delta \leqslant +80$, Al^{V}: $+25 \leqslant \delta \leqslant +45$ and Al^{VI}: $-20 \leqslant \delta \leqslant +20$).[20] Note that after the removal of the associated water and the organic residues the concentrations of Al^{IV} and Al^{V} increase at the expense of Al^{VI}.

In contrast to the unheated and the preheated sol–gel powders, respectively, the annealed samples (Fig. 5) show sharp signals indicating the presence of crystalline phases corresponding to the results of X-ray diffraction and DTA–TG. The pure samples show one sharp signal each at +5.6 ppm (1 annealed, pure tielite) and −13.2 ppm (4 annealed, pure hollandite) respectively. The tielite and potassium hollandite composite (3 annealed) gives two sharp signals at +4.4 ppm and −13.2 ppm. The slight difference of the chemical shift of the tielite phase in the pure and composite samples (+5.6 ppm *vs.* +4.4 ppm) is not significant since the experimental error of the chemical shift is *ca.* ±1 ppm.

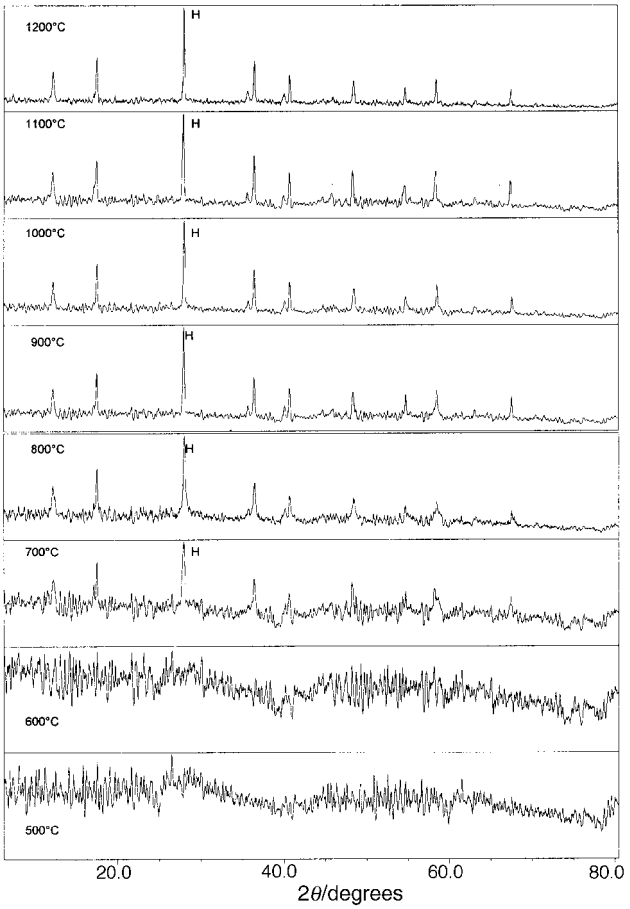

Fig. 3 X-Ray patterns of sol–gel powders 4 after annealing at 500–1200 °C for 48 h, each; H marks the strongest peak of potassium hollandite

SEM–EDX. EDX studies of the sol–gel powders and of the samples preheated at 500 °C, show no inhomogeneities with respect to the element distributions on the level of the lateral resolution of *ca.* 1 μm. The morphology of the sol–gel powders with a particle size of about 5–500 nm is shown in Fig. 6.

Fig. 7 and 8 clearly show the rod-shaped habitus of potass-

Table 3 Crystallisation and formation temperatures of the product phases from the sol–gel powders as detected by X-ray diffraction and by DTA–TG (in brackets)

batch	T:H	C (H)	C (K)	C (A)	C (R)	F (T)
1	1:0	—	800 °C (778 °C, 998 °C)	—	800 °C (778 °C, 998 °C)	1300°C (1350 °C)
3	3:1	800 °C (806 °C)	800 °C (806 °C)	700 °C (703 °C)	800°C (806 °C)	1400 °C —
4	0:1	700 °C (746 °C)	—	—	—	—

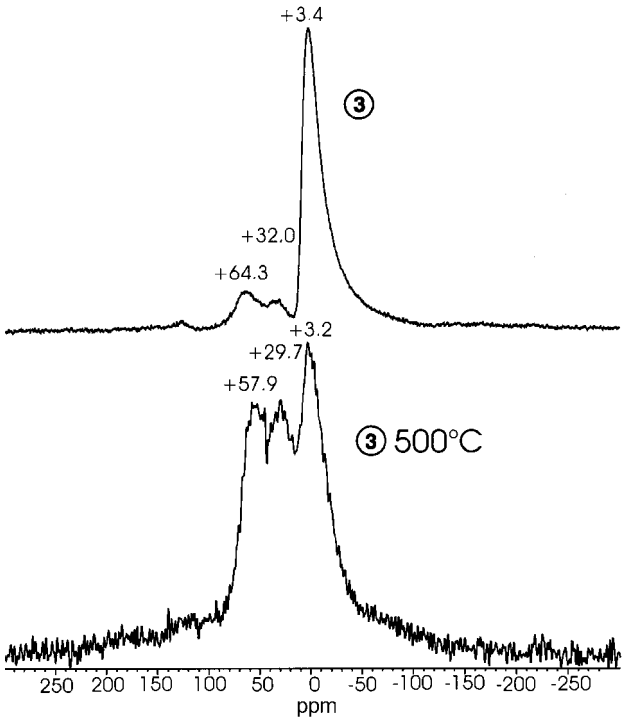

Fig. 4 ^{27}Al MAS NMR spectra of sol–gel powder 3 before and after heating at 500 °C

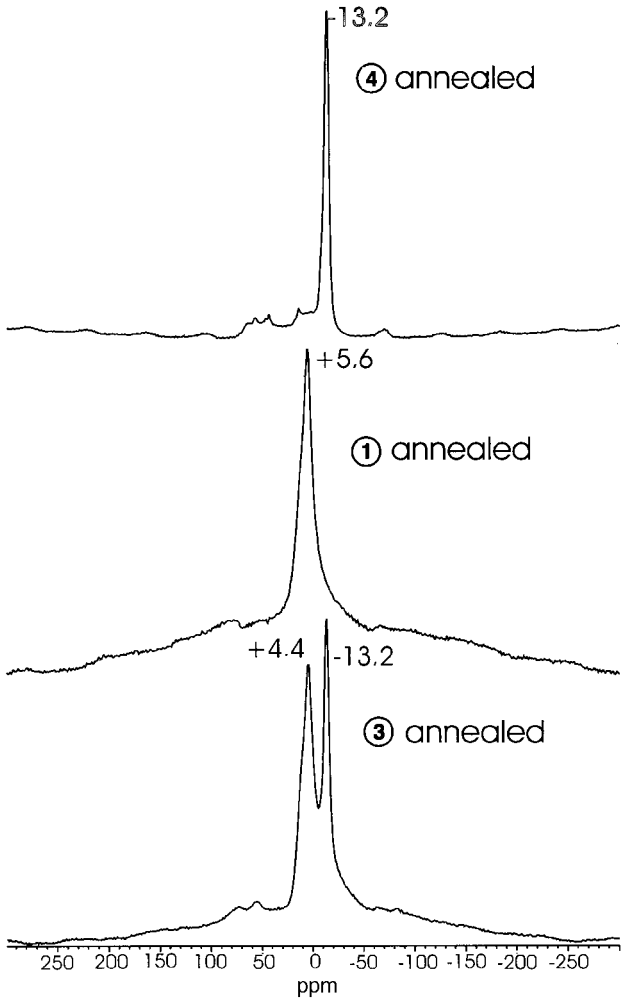

Fig. 5 ^{27}Al MAS NMR spectra of the annealed sol–gel powders 4, 1 and 3

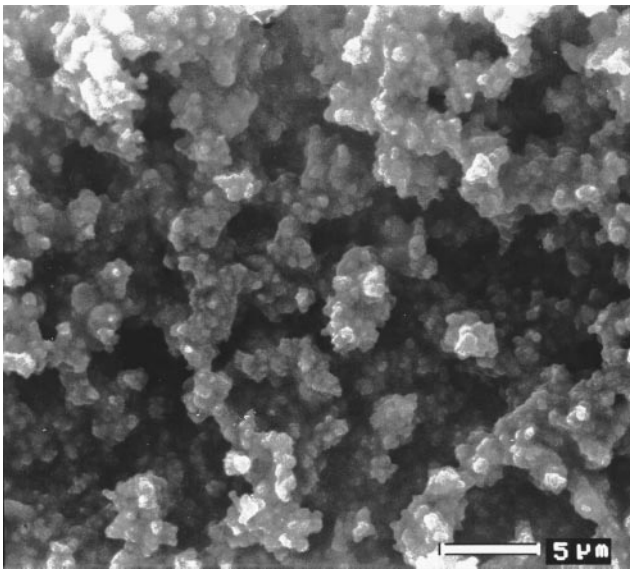

Fig. 6 Fine-grained texture of sol–gel powder 4 after heating at 500 °C for 48 h

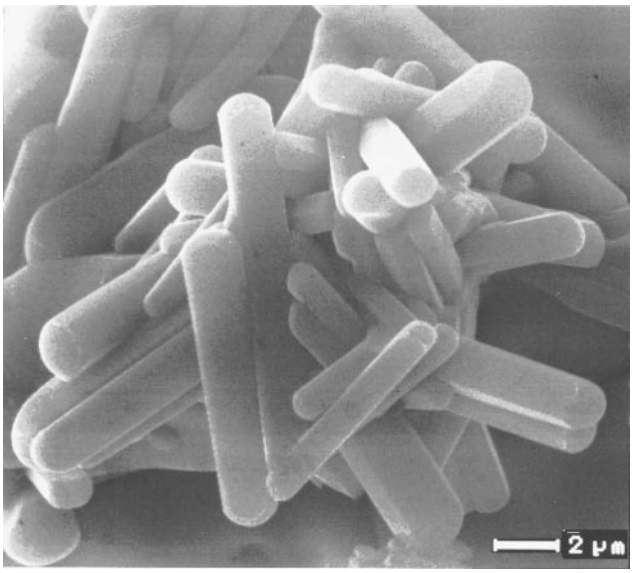

Fig. 7 Whisker-shaped crystals of the pure potassium hollandite phase (4 annealed)

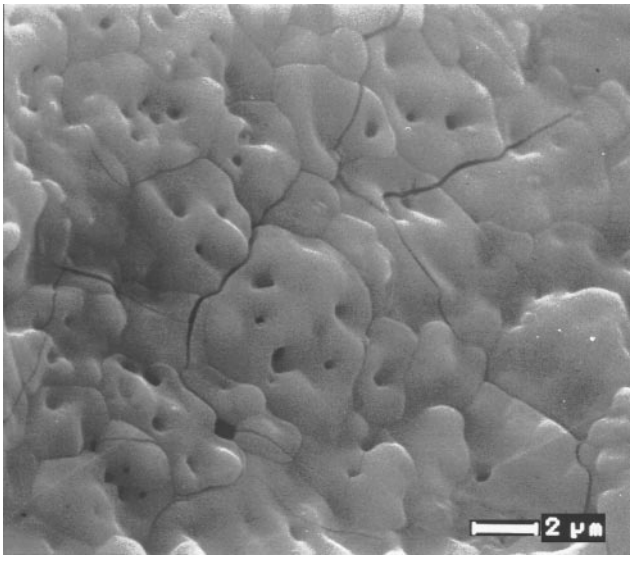

Fig. 8 Texture of the pure tielite phase (1 annealed)

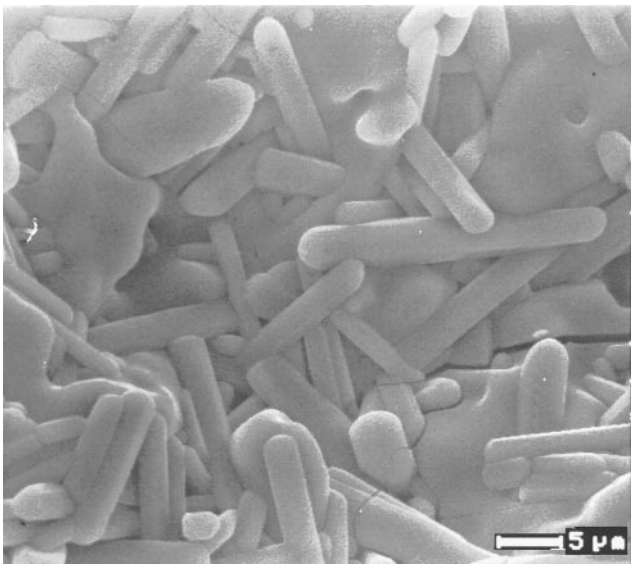

Fig. 9 Composite microstructure of sample 3 after annealing

ium hollandite and the typical micro holes and micro cracks of the pure tielite, respectively, as obtained by annealing the corresponding sol–gel samples. The hollandite needles have dimensions of 1–3 µm in diameter and 10–20 µm in length. Their angular and hexagonal habit indicates them to be single crystals, though this is still to be proven by transmission electron microscopy.

Fig. 9 demonstrates that a rod-shaped growth of potassium hollandite is also achieved within a tielite matrix. The dimensions of the needles and of the micro cracks, respectively, are in the same range as those in the pure potassium hollandite and in the pure tielite sample. The tight intergrowth of hollandite needles and the tielite matrix can be well observed at 5000-fold magnification (Fig. 10). The microstructure of the tielite rich sample 2 is shown in Fig. 11. EDX spot analyses confirm the compositions Al_2TiO_5 (tielite) and $K_2Al_2Ti_6O_{16}$ (potassium hollandite) of the two phases.

Reaction sintering

X-Ray diffraction. In order to determine the temperatures at which tielite and potassium hollandite form when starting from polycrystalline powders, batches of compositions as given in

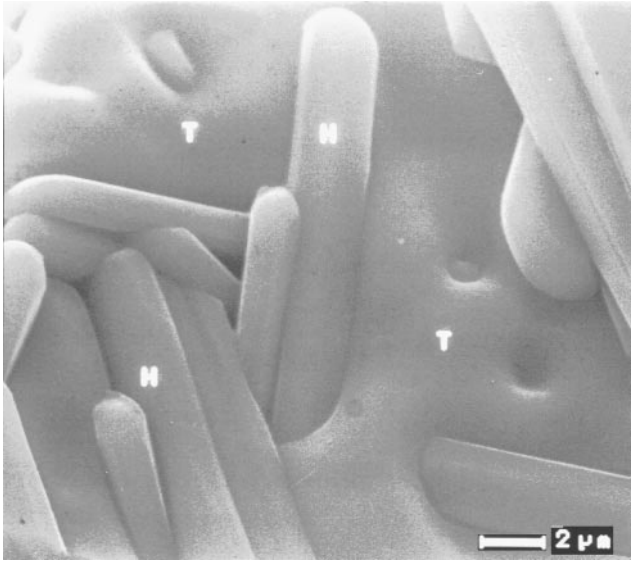

Fig. 10 Intergrowth of potassium hollandite whiskers and the tielite matrix (3 annealed)

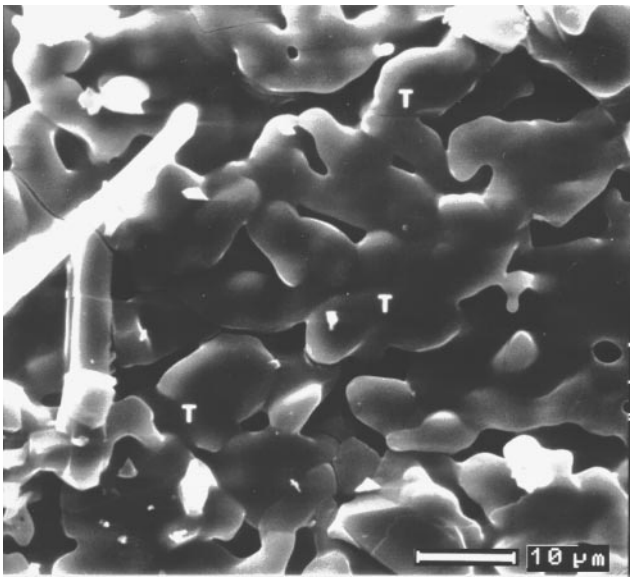

Fig. 11 Microstructure of the tielite rich sample 2

Table 2 were sintered at temperatures of 500–1480 °C and the reaction products analysed by X-ray diffraction. Fig. 12 shows the X-ray diffraction patterns of sample 4 as examples. First potassium carbonate reacts with rutile forming potassium titanate $K_2Ti_6O_{13}$[21] which then reacts with corundum at 1100 °C forming potassium hollandite $K_2Al_2Ti_6O_{16}$.

Sample 3 shows two significant differences compared to the pure hollandite and tielite batches. Firstly, the formation of

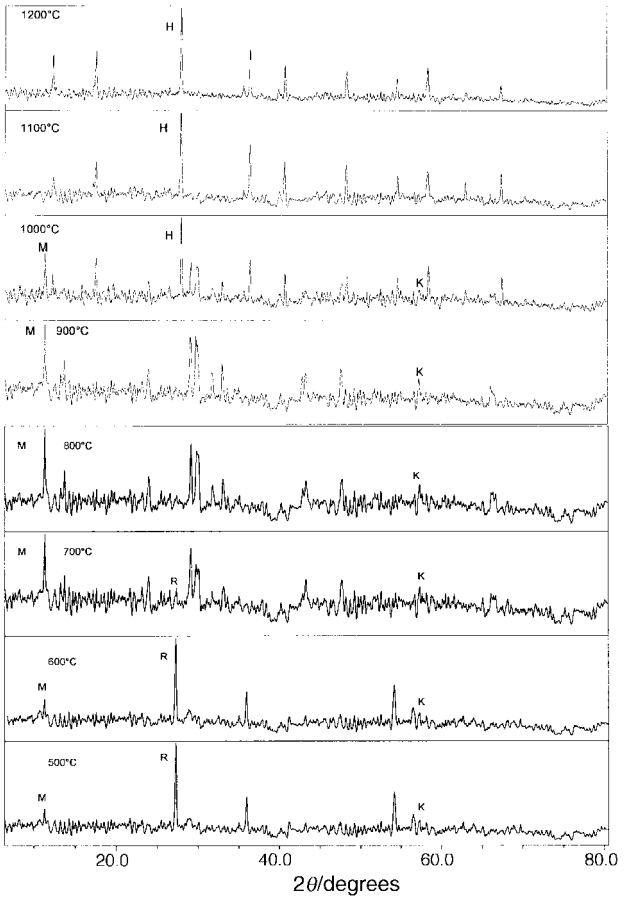

Fig. 12 X-Ray patterns of crystalline powder mixtures 4 after annealing at 500–1200 °C for 48 h, each; R, M, K and H mark the strongest peaks of rutile TiO_2, $K_2Ti_6O_{13}$, corundum Al_2O_3 and potassium hollandite, respectively

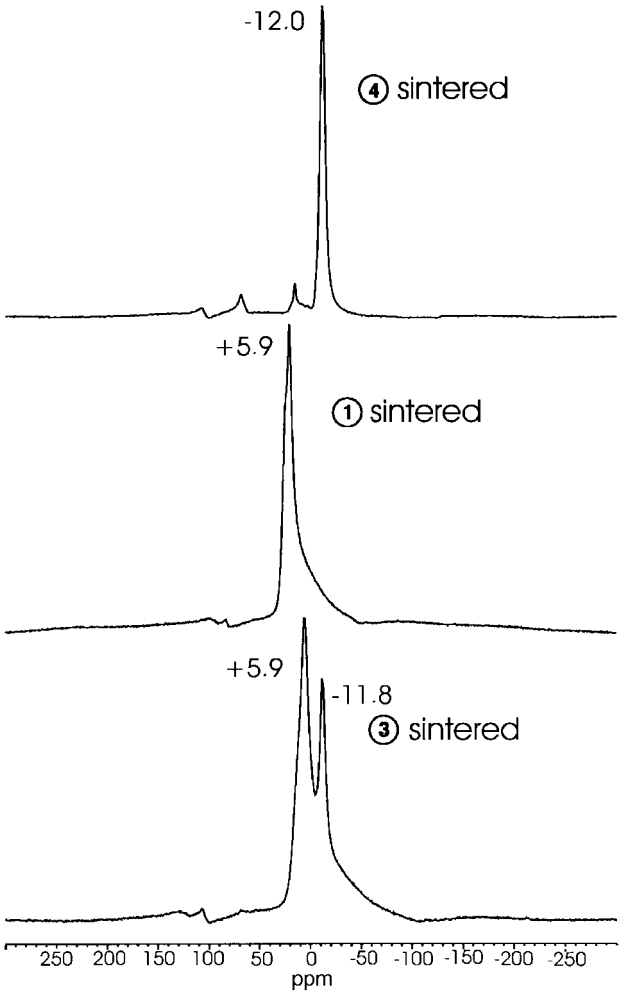

Fig. 13 ^{27}Al MAS NMR spectra of the reaction products as obtained by reaction sintering

potassium hollandite is already completed at 1000 °C. Secondly, the formation of tielite is not finished until heating to 1480 °C. The same trend was observed for the sol–gel powders.

^{27}Al MAS NMR spectroscopy. The sintered samples (Fig. 13) show sharp signals indicating the presence of crystalline phases in agreement with the X-ray diffraction results. The pure samples show sharp signals each at +5.9 ppm (1 sintered, pure tielite) and −12.0 ppm (4 sintered, pure hollandite). The tielite and potassium hollandite composite (3 annealed) gives two sharp signals at +5.9 ppm and −11.8 ppm. This corresponds to the results of the sol–gel process (Fig. 5). The slight differences of the chemical shifts are not significant.

SEM–EDX. According to the results of X-ray diffraction and NMR spectroscopy the samples obtained *via* the sol–gel route and by reaction sintering appear to be identical. Significant differences concerning the texture between the two tielite samples could not be detected. As shown in Fig. 14 a growth of rod-shaped crystals of potassium hollandite can also be achieved by reaction sintering. However, the shapes of the needles are slightly different, in particular the length/diameter ratio is smaller in the latter case. The hollandite needles have dimensions of 2–3 μm in diameter and 10–15 μm in length. As in the annealed sol–gel samples their angular and hexagonal habit indicates them to be single crystals, though this is only indirect evidence which is still to be proven by transmission electron microscopy.

The intergrowth of potassium hollandite whiskers and the tielite matrix yields a texture similar to that of the sol–gel derived samples (Fig. 15). Like in the pure sample the rod-shaped hollandite needles have dimensions of 2–3 μm in diameter and 10–15 μm in length.

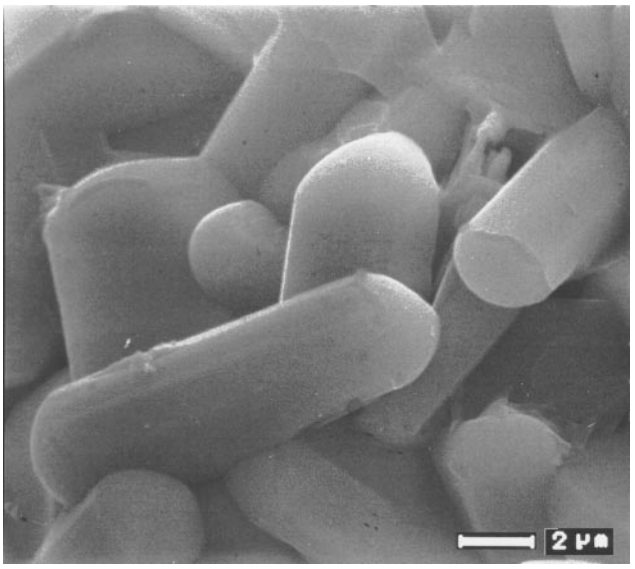

Fig. 14 Growth of basically whisker-shaped crystals of the pure potassium hollandite phase (4 sintered)

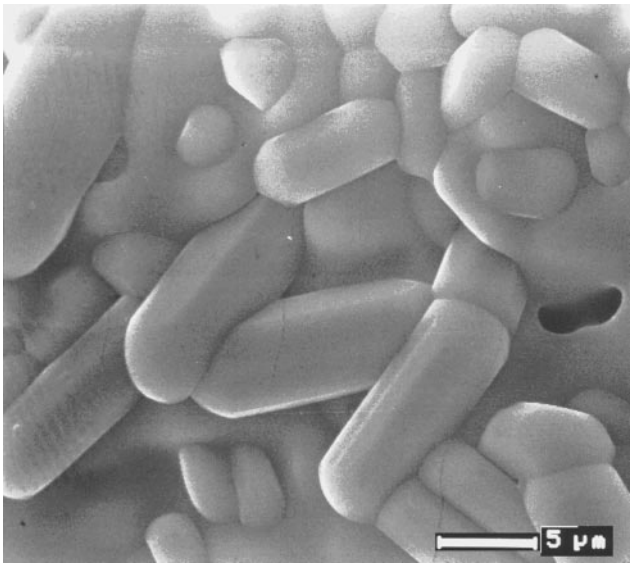

Fig. 15 Composite microstructure of sample 3 (sintered)

Glass ceramic process

In the dark-blue samples Magneli phases Ti_nO_{2n-1} can be detected by X-ray diffraction. This is caused by the partial release of oxygen from titanium dioxide at the elevated temperatures during the synthesis. The potassium containing samples show high potassium losses during the melting process through evaporation of K_2O. This was documented by EDX analyses and by determination of the samples' weight loss.

Thus the glass ceramic process in the quaternary system K–Al–Ti–O seems not to be applicable for the high melting compositions which, on the other hand, have to be considered if the preparation of a hollandite penetrated tielite ceramic (see Introduction, Fig. 1) is intended.

Summary and conclusion

The preparation of a tielite ceramic penetrated by potassium hollandite whiskers was achieved by internal precipitation.

Three different routes were studied: (1) a sol–gel process, (2) reaction sintering, and (3) a glass ceramic process.

Via sol–gel process and reaction sintering, the desired microstructures have been obtained, as has been proven by X-ray diffraction, ^{27}Al MAS NMR spectroscopy, DTA–TG and SEM–EDX. The results presented demonstrate that the general tendency of potassium hollandite $K_2Al_2Ti_6O_{16}$ to needle-shaped crystal growth can be used for whisker precipitation inside a solid matrix. Lengths and diameters are in the same order of magnitude as for some commercially available whiskers.[22] The microstructures of these ceramics still show the typical microcracks and microholes of tielite. The mechanical strength of the prepared ceramics has not been tested yet. However, the concept of internal whisker precipitation is shown to be principally feasible from a chemical point of view, and we intend to extend this concept to other ceramic systems.

For the system K–Al–Ti–O the glass ceramic process does not seem to be a promising approach due to evaporation of K_2O.

The authors gratefully acknowledge the financial support by the Deutsche Forschungsgemeinschaft (DFG), Bonn, especially within the Sonderforschungsbereich 408, and would like to thank Dr. Wilfried Hoffbauer for recording the ^{27}Al MAS NMR spectra and for discussing special problems of NMR spectroscopy.

References

1 W. Seidel, *Werkstofftechnik*, Carl Hauser Verlag, München, 1990, 1st edn.
2 P. K. Mehrotra and D. P. Ahuja, *Ceram. Eng. Sci. Proc*., 1992, **13,** 688.
3 A. Weber, *Werkstoffkunde*, VDI Verlag, Düsseldorf, 1989, 1st edn.
4 L. Wang, H. Wada and L. F. Allard, *J. Mater. Res*., 1992, **7**, 148.
5 G. Peters and M. Jansen, *Mat.-wiss. Werkstofftech*., 1994, **25**, 490.
6 E. N. Bunting, *J. Res. Natl. Bur. Stand*., 1933, **11**, 719.
7 E. Gugel and P. Schuster, *Tonind. Ztg*., 1974, **98**, 315.
8 B. Morosin and R. W. Lynch, *Acta Crystallogr., Sect B*, 1982, **28**, 1040.
9 D. D. Gulamova and M. K. Sarkisova, *Inorg. Mater*., 1989, **25**, 671.
10 S. M. Lang, C. L. Fillermore and L. H. Maxwell, *J. Res. Natl. Bur. Stand*., 1952, **48**, 298.
11 H. W. Hennicke and W. Lingenberg, *Ber. Dtsch. Keram. Ges*., 1986, **63**, 100.
12 W. P. Byrne, R. Morell and J. Lawson, *Sci. Ceram*., 1988, **14**, 775.
13 E. Kato, K. Daimon, J. Takahashi, R. Kato and K. Hamano, *Rep. Res. Lab. Eng. Mater*., 1984, **9,** 75.
14 T. Kameda (Toshiba Corp.), JP 01115687 A2; *Chem. Abstr*., 1989, **111,** 119853f.
15 S. E. Keeson and T. J. White, *Proc. R. Soc. London Ser. A*, 1986, **405**, 295.
16 T. H. White, R. L. Segall and P. S. Turner, *Angew. Chem*., 1985, **97**, 369.
17 J. Réau, J. Moali and P. Hagenmuller, *C. R. Acad. Sci. Paris Ser. C*, 1983, **284**, 655.
18 M. Watanabe and Y. Fujiki, *J. Solid State Chem*., 1987, **66**, 56.
19 R. W. Cheary, J. V. Hunt and P. Calaizis, *J. Aust. Ceram. Soc*., 1981, **17**, 11.
20 R. J. Kirkpatrick, in *Spectroscopic Methods in Mineralogy and Geology*, ed. F. C. Hawborne, *Mineral Soc. Am*., Washington DC, 1988.
21 E. Andersen, I. Andersen and E. Skou, *Solid State Ionics*, 1988, **27**, 181.
22 T. Kandori, S. Kobayashi, S. Wada and O. Kamigatio, *J. Mater. Sci. Lett*., 1987, **6**, 1356.

Paper 8/01304G; *Received* 16*th February*, 1998